Application of Raw and Chemically Modified Biomasses for Heterogeneous Cu-Catalysed Conversion of Aryl boronic Acids to Phenols Derivatives

Fernanda Guimarães Torres [1,2], Filipe Simões Teodoro [3], Leandro Vinícius Alves Gurgel [3], Flavien Bourdreux [2], Olfa Zayene [2], Anne Gaucher [2], Laurent Frédéric Gil [1,*] and Damien Prim [2,*]

[1] Group of Organic and Environmental Chemistry (GOEQ), Department of Chemistry, Institute of Biological and Exact Sciences, Federal University of Ouro Preto, Campus Morro do Cruzeiro, s/n°, Bauxita, Ouro Preto 35400-000, Minas Gerais, Brazil; fernanda.torres@aluno.ufop.edu.br

[2] Institut Lavoisier de Versailles, CNRS, UVSQ, ILV, Université Paris-Saclay, 78000 Versailles, France; flavien.bourdreux@uvsq.fr (F.B.); olfa.zayene@uvsq.fr (O.Z.); anne.gaucher@uvsq.fr (A.G.)

[3] Group of Physical Organic Chemistry (GPOC), Department of Chemistry, Institute of Biological and Exact Sciences, Federal University of Ouro Preto, Campus Morro do Cruzeiro Bauxita, Ouro Preto 35400-000, Minas Gerais, Brazil; filipe.teodoro@ufop.edu.br (F.S.T.); legurgel@ufop.edu.br (L.V.A.G.)

[*] Correspondence: laurent@ufop.edu.br (L.F.G.); damien.prim@uvsq.fr (D.P.)

Abstract: This work describes the application of raw and chemically modified cellulose and sugarcane bagasse for *ipso*-hydroxylation of aryl boronic acids in environmentally friendly reaction conditions. The catalytic efficiency of five support-[Cu] materials was compared in forming phenols from aryl boronic acids. Our investigation highlights that the CEDA-[Cu] material (6-deoxy-6-aminoethyleneamino cellulose loaded with Cu) leads to the best results under very mild reaction conditions. The optimized catalytic sequence, allowing a facile transformation of boronic acids to phenols, required the mandatory and joint presence of the support, Cu_2O, and KOH at room temperature. CEDA-[Cu] was characterized using ^{13}C solid-state NMR, ICP, and FTIR. The use of CEDA-[Cu] accounts for the efficacious synthesis of variously substituted phenol derivatives and presents very good recyclability after five catalytic cycles.

Keywords: cellulose; heterogeneous catalysis; *ipso*-hydroxylation; phenol; copper

1. Introduction

Due to the necessity to use renewable resources versus fossil resources, materials prepared from biomass, such as chitosan, sugarcane bagasse or cellulose, are of particular interest [1–4]. Recently, biopolymers such as cellulose have received tremendous global attention as a biodegradable, abundant, easy to modify, non-toxic solid support for metal catalysts [5,6]. In general, the polymer-surface modification through the introduction of new ligand-type fragments may result in the formation of different chelating sites, which can be used to produce new organic matrices [5]. If raw and modified cellulose are able to complex many metals as Cu [6], Pt [6,7], Pd [8,9], Co [10], and Mo [10], cellulose-[Cu] materials have garnered attention due to their versatile catalytic properties. Indeed, copper-catalysed transformations are part of the chemical toolbox available to the scientific community to increase molecular diversity and complexity. Among these, the *ipso*-hydroxylation of boronic acids represents one of the preparation routes to phenols. The scientific community's interest in this useful synthetic transformation arises from the wide occurrence of phenols in biologically active compounds, agrochemicals, synthetic intermediates, and polymers [11–17]. The access to phenols by *ipso*-hydroxylation of boronic acids can be achieved in three main ways including photocatalysis [18], the use of strong

oxidants [19–22], and the use of transition metals. Among the latter, Cu-catalysed synthesis of phenols from boronic acid precursors appears as a general and efficient procedure under both homogeneous [23] and heterogeneous catalysis using various solid supports including Cu_2O nanoparticles and banana pulp extracts [20], carbon nanotube-chitosan nanohybrid films [24], microheterogeneous biphasic systems [25], biogenic Cu_2O nanoparticles [26], Cu-Phen [23], $Cu(OH)_x$-Clay [27], $CuCl_2$-cryptand-[2.2.Benzo] [28], or modified chitosan [5,18,29]. However, these protocols may suffer from drawbacks such as longer reaction time, higher temperature, the use of organic solvents and oxidants, and lack of recyclability. Thus, the development of approaches combining concepts of green absorbent ability and capacity to promote organic transformations such as *ipso*-substitution of boronic acids under environmentally friendly conditions is a current major concern.

In this work, we investigated the application of five solid supports (Figure 1), including raw and modified cellulose and sugarcane bagasse as new heterogeneous catalysts for *ipso*-substitution of aryl boronic acids.
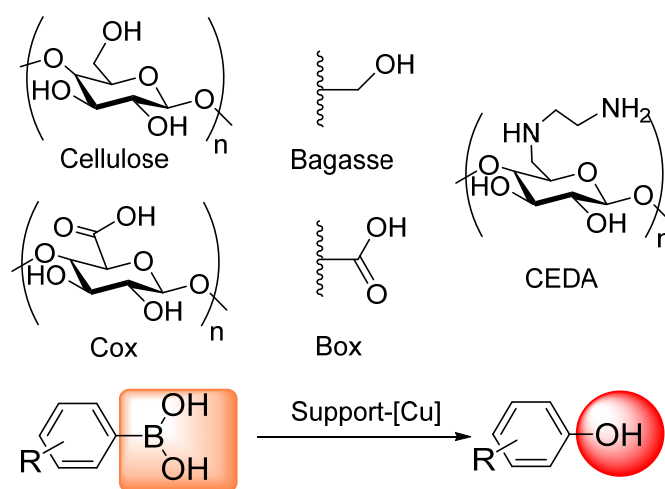

Figure 1. Bio-based solid supports: raw cellulose, oxidized cellulose (Cox), raw sugarcane bagasse, oxidized sugarcane bagasse (Box), 6-deoxy-6-aminoethyleneamino cellulose (CEDA) and *ipso*-hydroxilation of boronic acids.

2. Results and Discussion

If raw cellulose and sugarcane bagasse are commercially available biopolymers, Box and Cox must be prepared. The latter two chemically modified biopolymers have been easily obtained using oxidative procedures recently developed by us [4]. Similarly, CEDA is readily prepared from cellulose through a short one-pot two-step synthetic sequence involving tosylation followed by the addition of ethylenediamine as recently described [2].

CEDA-[Cu] was characterized by FTIR and ^{13}C MC-CP MAS NMR and the presence of Cu species in CEDA-[Cu] was quantified by ICP.

2.1. Fourier Transform Infrared Spectroscopy (FTIR)

Box and Cox materials have already been synthesized and characterized by our group [4]. In order to prove the formation of the CEDA-[Cu] material, the FTIR analysis of the cellulose, CEDA, and CEDA-[Cu] were performed and the spectra recorded were compared. The FTIR spectra for cellulose, CEDA, and CEDA-[Cu] are presented in Figure 2. By comparing the spectra of CEDA and cellulose, it was possible to notice some evident changes due to the introduction of ethylenediamine units into the cellulose structure, such as (i) the appearance of a band at 1573 cm^{-1}, corresponding to angular deformation of the N-H bond in primary amines, (ii) the appearance of a band related to the stretching of the C-N bond overlapped in the 1240–1064 cm^{-1} region, and (iii) the appearance of a band at 813 cm^{-1} corresponding to out-of-plane bending of N-H bond [2].
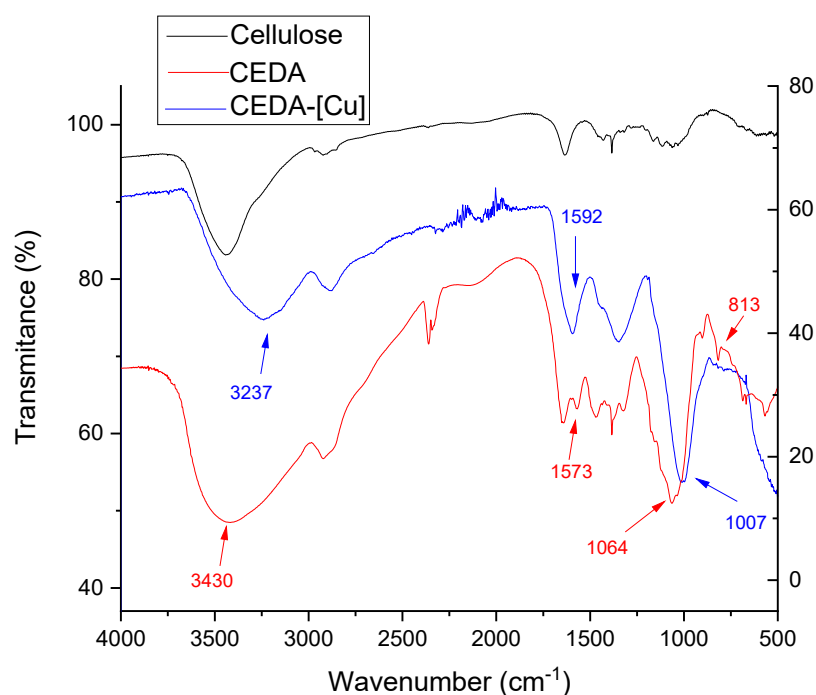
Figure 2. FTIR spectra of cellulose, CEDA, and CEDA-[Cu].

It was important to obtain the FTIR spectra of CEDA and CEDA-[Cu] to prove the presence of copper in the matrix and show the influence of the presence of the metal in the displacement and/or change of the absorption IR bands. The CEDA-[Cu] spectrum shows displacement and decrease in intensity of the band at 3237 cm^{-1} corresponding to the symmetric and asymmetric stretching of the N-H bond (primary and secondary amine), compared to the band at 3430 cm^{-1} for the CEDA IR spectrum. The complexation of Cu by CEDA caused (i) the displacement of the band related to angular deformation of the amine group (NH_2) from 1573 cm^{-1} to 1592 cm^{-1}, (ii) the displacement of the band corresponding to the stretching of the C-N bond from 1064 cm^{-1} to 1007 cm^{-1}, and (iii) the widening of the bands related to the formation of mono- and bidentate complexes with Cu^+ and Cu^{2+} compared to the CEDA IR spectrum.

2.2. ^{13}C Solid-State Nuclear Magnetic Resonance (^{13}C SS NMR)

As shown in our previous work [3], ^{13}C MC-CP MAS NMR represents an accurate characterization technique in the solid-state allowing the quantitative determination of the grafting ratio [30] (unmodified cellulose vs. vicinal diamine-substituted solid support). Thus, the chemical structure of CEDA was investigated by ^{13}C MC-CP MAS NMR spectroscopy. The corresponding NMR spectrum is shown in Figure 3. Comparison with literature data on cellulose [31–33] allowed unambiguous attribution of characteristic vicinal diamine fragment.

Indeed, the NMR spectrum clearly shows the presence of signals corresponding to the vicinal diamine fragment carbon atoms 8 (50.5 ppm) and 9 (41.0 ppm). If carbon 6 of the unmodified subunit appears at 62.2 ppm, carbon 7 of the vicinal diamine fragment undergoes an expected upfield shift due to the presence of the neighbouring nitrogen atom. In addition, the ^{13}C MC-CP MAS NMR ^{13}C-NMR quantitative spectrum accounts for the determination of the grafting ratio. CEDA displays a 2:1 ratio between the unmodified subunit (*n* = 0.67) and the functionalized subunit (*m* = 0.33).

In an attempt to gain more information on the capacity of the vicinal fragment to accommodate Cu species, the classical CPMAS sequence was employed on CEDA-[Cu]. Unfortunately, the paramagnetic properties of the complexed Cu species generated a fast relaxation process of the carbons near the metal, preventing a quantitative analysis. As a

result, only the disappearance or decrease of the corresponding signals can be observed, allowing a qualitative comparison of the structural modifications between CEDA and CEDA-[Cu] (Figure 4). Classical CPMAS sequences ^{13}C-NMR undoubtedly showed that signals of C7, C8, and C9 were impacted by the proximity of the Cu species, evidencing the formation of the expected Cu complex in agreement with recent works dealing with paramagnetic Cu-complexes [34].
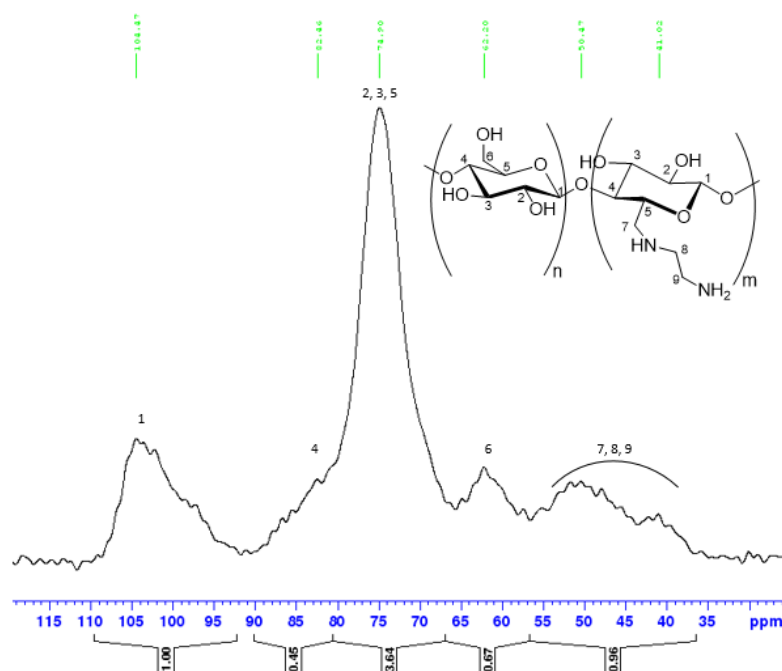

Figure 3. Quantitative ^{13}C-NMR spectrum of CEDA.

2.3. Ipso-Hydroxylation of Boronic Acids

We started our investigations based on the recent work by Kim et al. [5] dealing with hydroxylation of boronic acids using modified chitosan as solid support. In this work, experimental conditions were thoroughly studied and optimized. Best results were obtained using Cu_2O and KOH in water at room temperature for 24 h.

We used these conditions to initiate our own study. First, we focused on phenyl boronic acid to compare several biopolymers as the support and identify the most efficient one. Second, we determined the optimum reaction time for 4-bromo phenyl boronic acid transformation to 4-bromophenol. Indeed, the study of *ipso*-hydroxylation in the presence of a bromine atom on the substrate might represent a challenge under transition metal catalytic conditions and its preservation after transformation, an opportunity for further functionalizations on the aromatic ring.

Four different supports have been tested under the same set of conditions (Cu_2O, KOH 3 eq., H_2O, rt, O_2, 24 h). As shown in Table 1, raw cellulose and sugarcane bagasse afforded only partial conversion, the starting phenylboronic acid **1** and the starting phenyl-boronic acid 1 remained the crude product's major component (entries 1 and 2). Rates have been determined by integrating characteristic ^{1}H-NMR signals of ortho protons of both the reactant (8.26 ppm) and the product (6.86 ppm). Oxidized solid supports such as Cox and Box behaved differently. The use of Cox (entry 3) did not afford any conversion after 24 h. In contrast, Box showed an enhanced reactivity by comparison with raw sugarcane bagasse, allowing obtaining phenol **2** as the major product in a 1/1.2 ratio (entry 4). Interestingly, CEDA afforded under identical conditions a complete conversion, as no traces of the starting boronic acid could be detected in the crude material ^{1}H-NMR (entry 5). Control experiments ran alternatively without KOH (entry 6) or Cu_2O (entry 7), which led the starting boronic acid to be unchanged after 24 h. It is worth noting that cellulose, bagasse,

and Box behaved similarly under complementary control experiments. In conditions C, no conversion of the starting boronic acid could be observed.
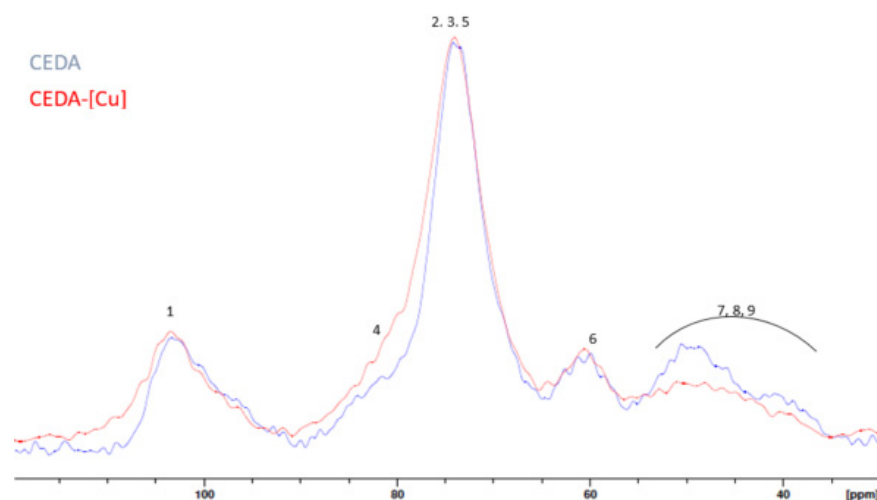

Figure 4. Comparison of CPMAS ^{13}C-NMR of CEDA and CEDA-[Cu].

As a result, the combined presence of both reactants is mandatory to the *ipso*-hydroxylation process. Interestingly, in the absence of CEDA (entry 8), *ipso*-hydroxylation occurred, although it led to a modest 1/0.5 ratio of phenylboronic acid to phenol. This result shows that (i) the presence of the vicinal diamine unit is essential to achieve complete conversion; (ii) the joint presence of Cu_2O, KOH, and CEDA provides a relevant catalytic system for hydroxylation of boronic acids; (iii) the plausible formation of a (*N,N*)Cu complex within the solid support helps to exacerbate the reactivity of the catalytic active species, giving rise to increased rate and completion of the reaction. Attempting to decrease the reaction time to 7 h instead of 24 h afforded a modest reactant to product ratio of 1:1.2 (entry 9), which led us to examine the evolution of the ratio with time. To this end, we further investigated the *ipso*-hydroxylation process of valuable 4-bromophenylboronic acid **3** under the conditions mentioned above at room temperature by varying the reaction time.

Four identical reactions were carried out using Cu_2O, KOH, and H_2O at room temperature. The reaction mixtures were filtrated at 7, 14, 19, and 24 h. Filtrates were subjected to classical workup (see experimental section) and ^{1}H-NMR to determine 3/4 ratio. As shown in Figure 5, after 7 h, 2/3 of the starting boronic acid was converted into the corresponding phenol derivative. The proportion of **4** in the crude reaction mixture increases after 14 h, then after 19 h until obtaining a complete conversion of **3** in 24 h. Further, 4-bromophenol **4** could be isolated in 41, 81, and 93% and quantitative yields at 7, 14, 19, and 24 h reaction course, respectively.

Increasing temperature from rt to 40 °C and further 60 °C allowed complete consumption of the starting material in 5 h. However, under such conditions, the presence of biphenyl, most likely arising from a homocoupling of boronic acid, was also detected decreasing the yield of expected phenol [23,35]. Thus, the substrate scope was examined at room temperature for 24 h.

Under the optimized conditions, a range of aryl boronic acids were subjected to the hydroxylation process and the results were gathered in Figure 6. Methyl cresols **5** and **6** as well as the 2,4-xylenol **7** were isolated in good 54, 72, and 83% yields, respectively. Interesting results have been obtained for phenyl boronic acids bearing methoxy substituents, leading to the corresponding phenols **9** and **10** in high yields, except for the ortho substituted pattern, which did not afford the expected guaiacol **8**. Hydroquinone **12** bearing two hydroxyl functions has been isolated in 90% yield. In contrast, *ortho*-bromophenol **11** was isolated in a poor 9% yield. Attempts to prepare the expected phenol **13** remained unsuccessful since the nucleophilic substitution of the benzylic bromine competes favourably to the

ipso-hydroxylation process. α and β-naphthols **14** and **15** have been isolated in fair 47 and 51% yields, respectively. It is worth noting that attempts to transform higher polycyclic aromatic hydrocarbon boronic acids, such as anthracene, phenanthrene or pyrene failed under these conditions. Boronic acids located at π-deficient heterocycle such as pyrimidine **16** or substituted electron-withdrawing group such as CF₃ **17** failed to undergo the hydroxylation process.

Table 1. Determination of most suitable solid support and catalytic system.
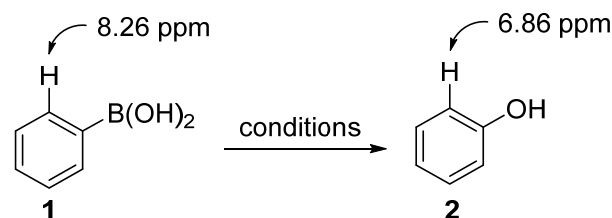
Entry	Solid Support	Conditions	Time (h)	Ratio 1/2 [a]
1	Cellulose	A	24	1/0.8
2	Bagasse	A	24	1/0.5
3	Cox	A	24	1/0
4	Box	A	24	1/1.2
5	**CEDA**	**A**	**24**	**0/1**
6	CEDA	B	24	1/0
7	CEDA	C	24	1/0
8	-	D	24	1/0.5
9	CEDA	A	7	1/1.2

Conditions A: solid support, Cu₂O, KOH 3 eq., H₂O, rt, O₂ ballon; Conditions B: condition A without KOH; Conditions C: condition A without Cu₂O; Conditions D: condition A without solid support; [a] ratio determined by ¹H-NMR.
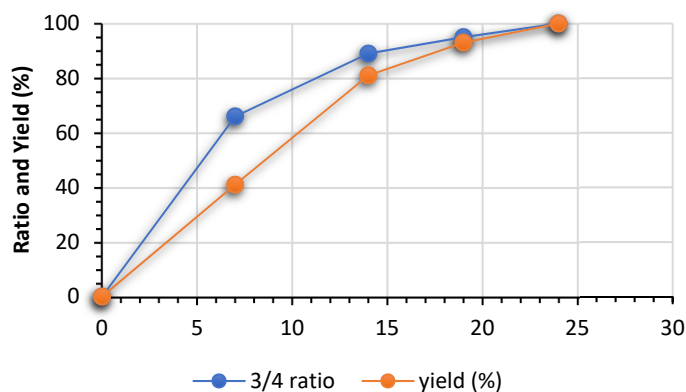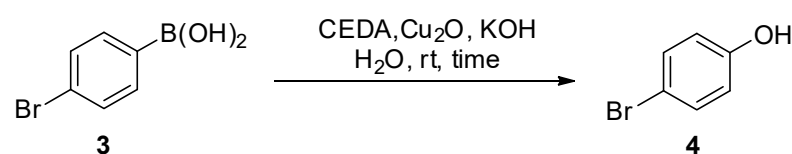
Figure 5. Optimization of reaction time using CEDA-[Cu]. In blue dots/line, the ratio determined by ¹H-NMR. In orange dots/line isolated yields.
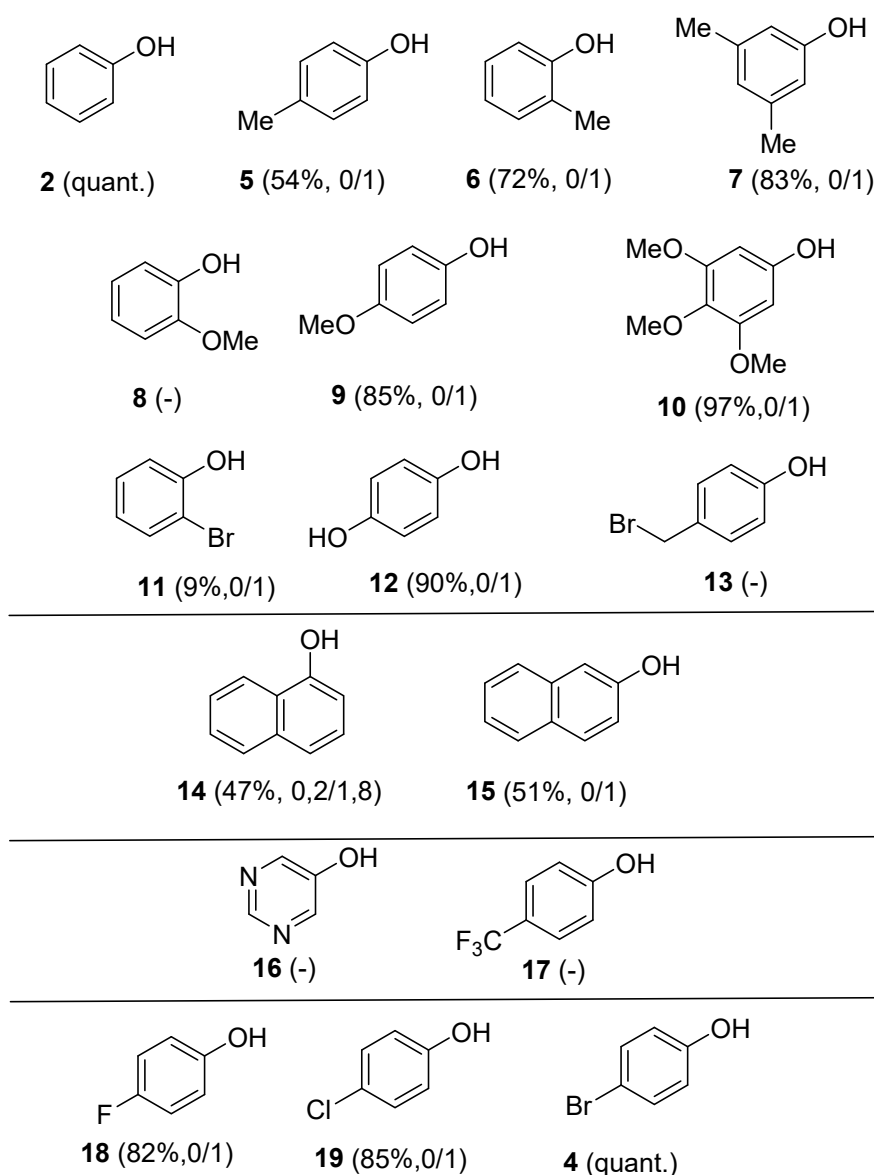
Figure 6. Substrate scope (isolated yields, ratio starting material/product).

Finally, *para* fluoro, chloro, and bromo phenylboronic acids were also tested. Interestingly, the presence of halogen atoms did not hamper the hydroxylation process, giving rise to a chemoselective metal-catalysed hydroxylation. The corresponding fluoro, chloro, and bromo phenols **18**, **19**, and **4** were isolated in 82% to quantitative yields.

Copper-based catalytic systems in water have been shown to be recyclable for the obtention of various functional groups from aryl boronic acids [36]. Our next goal was thus to test the recyclability of our material. The experimental workup of the classical hydroxylation process implies the filtration and washings of the CEDA-[Cu] heterogeneous catalytic system. After filtration, the CEDA-[Cu] was dried at 50 °C overnight and used again for a further run. We decided to test the recyclability with 4-bromophenylboronic acid. Cu contents after each run have been determined using ICP-OES.

As shown in Figure 7, we observed a slight erosion of yields from quantitative in the first run to 82% in cycle number 5. This erosion parallels the moderate decrease of the Cu content of the catalytic system determined by the ICP measurements. Therefore, this trend could be attributed to the weak leaching of Cu species from the solid support and not a loss of catalytic activity. A control experiment using 8% loading of Cu_2O afforded the expected phenol in nearly 74% yield, confirming that erosion of yields observed is due

to the leaching phenomenon. Our heterogeneous Cu-based catalytic system appears thus robust after five runs and compares favourably to recent reports [5].
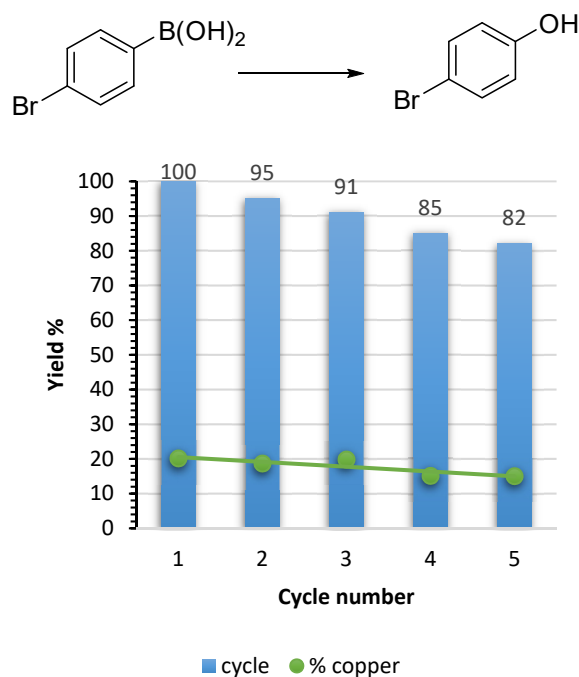

Figure 7. The evolution of catalytic process efficiency and CEDA-[Cu] reuse.

Although the mechanism of the *ipso*-hydroxylation of boronic acids is still being debated at this time [26], our experiments and observations strongly support a potential catalytic cycle involving (i) the intervention of Cu species early in the catalytic cycle and coordination of copper to the aryl boronic acid towards intermediate **A** [37]; (ii) the transformation into boronate complex **B** in basic medium [22,38]; (iii) migration of the aryl group towards **C** followed by hydrolysis and generation of **D** and boric acid $B(OH)_3$; and (iv) reductive elimination releasing the phenol derivative [35] (Figure 8).
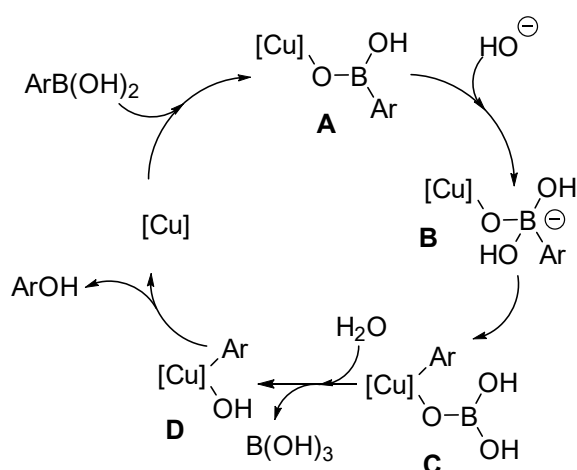

Figure 8. Proposed catalytic cycle.

3. Materials and Methods

3.1. Materials

Microcrystalline cellulose (Avicel PH-101), LiCl, triethylamine (TEA), and tosyl chloride (TsCl), Phenylboronic acid (97%), 4-Methylbenzeneboronic acid (98%), 4-hydroxybenzeneboronic acid (97%), 4-(Bromomethyl)phenylboronic acid (95%), 2-Naphthylboronic acid

(95%), 1-Naphthylboronic acid (95%), 4-(Trifluoromethyl)phenylboronic acid (95%), 4-chlorophenylboronic acid (95%), 4-bromophenylboronic acid (95%), 4-fluorobenzeneboronic acid (95%) were purchased from Sigma-Aldrich (San Luis, MO, USA). *N,N*-dimethylacetamide (DMA) and ethylenediamine (EDA) were purchased from Dinâmica Química Contemporânea (Indaiatuba, Brazil). HCl, Cu_2O, and $CaCl_2$ were purchased from Vetec (São Paulo, Brazil). Acetone, and diethyl ether were purchased from Synth (Suzano, Brazil). NaOH and ethanol, were purchased from Neon (Suzano, Brazil). 4-Methylbenzeneboronic acid (98%) was purchased from Alfa-Aesar (Haverhill, MA, EUA). 3,5-Dimethylphenylboronic acid was purchased from Maison (Xinji City, China). 3,4,5-Trimethoxyphenylboronic acid was purchased from Fluorochem (Hadfield, UK). 3,4,5-Trimethoxyphenylboronic acid was purchased from Acros (Pittsburgh, PA, USA). 2-Methoxyphenylboronic acid (99%) was purchased from Carlo (Val de Reuil, France). 5-Pyrimidinylboronic acid, (97%) was purchased from Maybridge (Altrincham, UK). Thin-layer chromatography (TLC) was carried out on aluminium sheets precoated with silica gel plates (Fluka Kiesel gel 60 F254, Merck Company, (Kenilworth, NJ, USA)) and visualized by a 254 nm UV lamp and potassium permanganate. ^{1}H-NMR analysis of compounds **7–9**, **11–14**, **16–17**, and **21–23** was in agreement with commercially available samples.

The ratio between starting boronic acids and phenol derivatives was determined by integrating ^{1}H-NMR signals. Unless otherwise stated, yields are isolated yields.

3.2. Methods

3.2.1. Synthesis of Cox and Box

Raw cellulose and sugarcane bagasse were oxidized with an H_3PO_4-$NaNO_2$ mixture to obtain Cox and Box, respectively. The optimized oxidation conditions for the preparation of Cox and Box are described in our previous work [4].

3.2.2. Synthesis of CEDA

The solid support CEDA was prepared by tosylation of microcrystalline cellulose followed by nucleophilic substitution of the tosyl group by ethylenediamine. CEDA was produced as described in our previous work [2].

3.2.3. Synthesis of CEDA-[Cu]

A round-bottom flask (25 mL) was charged with 0.500 g of CEDA, 0.1 mmol of Cu_2O, 3.0 mmol of KOH, and 5 mL of H_2O. The mixture was stirred at room temperature for 24 h. At the end of the reaction, the mixture was vacuum filtered and washed with H_2O. The solid was dried and powdered.

3.2.4. Representative Procedure for *Ipso*-Hydroxylation of Boronic Acids

The procedures for the *ipso*-hydroxylation of arylboronic acids were adapted from Joo et al. [5]. A round-bottom flask (25 mL) was loaded with 1 mmol of arylboronic acid, 0.1 mmol of Cu_2O, 0.500 g of CEDA, 3.0 mmol of KOH, and 5 mL of H_2O. The mixture was stirred at room temperature in O_2 atmosphere for 24 h. At the end of the reaction the mixture was vacuum filtered and washed with H_2O. The solid was dried and stored, the filtrate was acidified with HCl solution until pH 2 and extracted with diethyl ether (3×10 mL). The combined organic layer was dried over anhydrous Na_2SO_4, then the solvent was evaporated under reduced pressure and the residue was diluted in chloroform for the ^{1}H-NMR analysis. Conversions were determined by ^{1}H-NMR of the crude reaction mixture. When necessary, mixtures of boronic acids and phenols were purified by chromatography on silica gel (cyclohexane) to afford the desired phenol derivative.

3.2.5. Preparation of Samples for Fourier Transform Infrared Spectroscopy (FTIR)

Samples for infrared analysis were prepared by mixing 2 mg of dry powder of cellulose, CEDA or CEDA-[Cu] with 100 mg of spectroscopy grade KBr. 13-mm diameter pellets were obtained by pressing the mixture in a hydraulic press at 6 tons (Pike CrushIR, model

181–1110). The FTIR spectrum was recorded on an ABB Bomen MB 3000 FTIR spectrometer (Quebec, Canada), with the detector set at a resolution of 4 cm^{-1} from 400 to 4000 cm^{-1} and 32 scans per sample.

3.2.6. ^{13}C Solid-State Nuclear Magnetic Resonance (^{13}C SS NMR)

CEDA was characterized by ^{13}C SS NMR spectroscopy, using the magic angle spinning (MAS) and multiple-contact cross-polarization (MC-CP) methods, performed with a Bruker NEO 500 MHz WB spectrometer. The ^{13}C CP-MAS NMR spectra were recorded using a static magnetic field of 11.7 T, at which ^{1}H and ^{13}C resonate at 500.16 and 125.76 MHz, respectively. The sample was packed in 4 mm outer diameter zirconia rotors and spun at 10 kHz. For tosyl cellulose (TsCel), a spectrum was recorded using MC-CP NMR, which has been shown to provide quantitative ^{13}C-NMR spectra for chitosan derivatives [3]. Seven CP contacts of 1.1 ms each were applied, separated by 0.5 s repolarization periods. In addition, ^{13}C CP-MAS NMR spectra were recorded. The ^{13}C radiofrequency (RF) field was set to 50 kHz. For the ^{1}H spectra, a 100–80% ramped amplitude.

3.2.7. ^{1}H Nuclear Magnetic Resonance (^{1}H-NMR)

^{1}H-NMR spectra of reaction products were recorded at 300 MHz and 298 K, using a spectrometer Bruker AVANCE I referenced to the tetramethylsilane (TMS) signal and was calibrated using residual CHCl$_3$ (δ = 7.26 ppm). ^{1}H-NMR spectroscopic data were reported as chemical shift δ (ppm) (multiplicity, coupling constant (Hz) and integration).

3.2.8. ICP Analysis

ICP measurement were performed using an Agilent ICP-OES 720 series. Samples were digested in 1 mL nitric acid for 24 h and then diluted to 40 mL with ultrapure water. The measures were performed at two wavelengths (327.395 and 324.754 nm) and repeated 9 times each.

4. Conclusions

We have developed a reusable and heterogeneous Cu-based catalyst system to prepare phenol derivatives from aryl boronic acids efficiently. Comparison of five raw and chemically modified biopolymers, including cellulose, bagasse, Box, Cox, and CEDA was carried out and CEDA-[Cu] was identified as the most efficient heterogeneous catalytic solid support. CEDA-[Cu] was characterized using ^{13}C solid-state NMR, ICP-OES, and FTIR. The optimized experimental conditions imply the solid support, Cu$_2$O, KOH joint presence in an aqueous medium. The synthetic transformation occurred smoothly at room temperature to afford variously substituted phenol derivatives in good to quantitative yields. The recyclability of CEDA-[Cu] has been investigated and allows its reuse up to five cycles with a minor loss of efficiency.

References

1. Gonçalves, F.; Gurgel, L.V.A.; Soares, L.C.; Teodoro, F.S.; Ferreira, G.M.D.; Coelho, Y.L.; da Silva, L.H.M.; Prim, D.; Gil, L.F. Application of pyridine-modified chitosan derivative for simultaneous adsorption of Cu(II) and oxyanions of Cr(VI) from aqueous solution. *J. Environ. Manag.* **2021**, *282*, 111939. [CrossRef] [PubMed]
2. Pereira, A.R.; Soares, L.C.; Teodoro, F.S.; Elias, M.M.C.; Savedra, R.M.L.; Siqueira, M.F.; Martineau-Corcos, C.; da Silva, L.H.M.; Prim, D.; Gurgel, L.V.A. Aminated cellulose as a versatile adsorbent for batch removal of As(V) and Cu(II) from mono- and multicomponent aqueous solutions. *J. Colloid Interface Sci.* **2020**, *576*, 158–175. [CrossRef]
3. Gonçalves, F.J.; Kamal, F.; Gaucher, A.; Gil, R.; Bourdreux, F.; Martineau-Corcos, C.; Gurgel, L.V.A.; Gil, L.F.; Prim, D. Synthesis, characterization and application of pyridine-modified chitosan derivatives for the first non-racemic Cu-catalysed Henry reaction. *Carbohydr. Polym.* **2018**, *181*, 1206–1212. [CrossRef] [PubMed]
4. Martins, L.R.; Rodrigues, J.A.V.; Adarme, O.F.H.; Melo, T.M.S.; Gurgel, L.V.A.; Gil, L.F. Optimization of cellulose and sugarcane bagasse oxidation: Application for adsorptive removal of crystal violet and auramine-O from aqueous solution. *J. Colloid Interface Sci.* **2017**, *494*, 223–241. [CrossRef]
5. Joo, S.-R.; Kwon, G.-T.; Park, S.-Y.; Kin, S.-H. Chemically Modified Chitosan as a Biopolymer Support in Coppercatalyzed *ipso*-Hydroxylation of Arylboronic Acids in Water. *Bull. Korean Chem. Soc.* **2019**, *40*, 465–468. [CrossRef]
6. Keshipour, S.; Shaabani, A. Copper(I) and palladium nanoparticles supported on ethylenediamine-functionalized cellulose as an efficient catalyst for the 1,3-dipolar cycloaddition/direct arylation sequence. *Appl. Organomet. Chem.* **2014**, *28*, 116–119. [CrossRef]
7. Islam, T.; Rosales, J.A.; Saenz-Arana, R.; Ghadimi, S.J.; Noveron, J.C. Rapid synthesis of ultrasmall platinum nanoparticles supported on macroporous cellulose fibers for catalysis. *Nanoscale Adv.* **2019**, *1*, 2953–2964. [CrossRef]
8. Prekob, Á.; Hajdu, V.; Muranszky, G.; Fiser, B.; Sycheva, A.; Ferenczi, T.; Viskolcz, B.; Vanyorek, L. Application of carbonized cellulose-based catalyst in nitrobenzene hydrogenation. *Mater. Today Chem.* **2020**, *17*, 100337. [CrossRef]
9. Li, D.-D.; Lu, G.-P.; Cai, C. Modified cellulose with tunable surface hydrophilicity/hydrophobicity as a novel catalyst support for selective reduction of nitrobenzene. *Catal. Commun.* **2020**, *137*, 105949. [CrossRef]
10. Santi, D.; Trisunaryanti, W.; Falah, I.I. Hydrocracking of pyrolyzed α-cellulose to hydrocarbon over MxOy/Mesoporous carbon catalyst (M = Co and Mo): Synthesis and characterization of carbon-based catalyst support from saw waste of Merbau wood. *J. Environ. Chem. Eng.* **2020**, *8*, 103735. [CrossRef]
11. Zhou, Y.; Ma, Z.; Tang, J.; Yan, N.; Du, Y.; Xi, S.; Wang, K.; Zhang, W.; Wen, H.; Wang, J. Immediate hydroxylation of arenes to phenols via V-containing all-silica ZSM-22 zeolite triggered non-radical mechanism. *Nat. Commun.* **2018**, *9*, 2931. [CrossRef] [PubMed]
12. Wang, W.; Li, N.; Shi, L.; Ma, Y.; Yang, X. Vanadium-zirconium catalyst on different support for hydroxylation of benzene to phenol with O$_2$ as the oxidant. *Appl. Catal. A* **2018**, *553*, 117–125. [CrossRef]
13. Tyman, J.H.P. *Synthetic and Natural Phenols*, 1st ed.; Elsevier Science: Amsterdam, The Netherlands, 1996; Volume 52, pp. 1–700. [CrossRef]
14. Rappoport, Z. *The Chemistry of Phenols*, 1st ed.; John Wiley and Sons: Oxford, UK, 2003; pp. 1–1667.
15. Quideau, S.; Deffieux, D.; Douat-Casassus, C.; Pouysegu, L. Plant polyphenols: Chemical properties, biological activities, and synthesis. *Angew. Chem. Int. Ed. Engl.* **2011**, *50*, 589–621. [CrossRef] [PubMed]
16. Ji, Y.; Li, P.; Zhang, X.; Wang, L. Trace amount Cu (ppm)-catalyzed intramolecular cyclization of 2-(*gem*-dibromovinyl)phenols(thiophenols) to 2-bromobenzofurans(thiophenes). *Org. Biomol. Chem.* **2013**, *11*, 4095–4101. [CrossRef] [PubMed]
17. Owen, R.W.; Giacosa, A.; Hull, W.E.; Haubner, R.; Spiegelhader, B.; Bartsch, H. The antioxidant/anticancer potential of phenolic compounds isolated from olive oil. *Eur. J. Cancer* **2000**, *36*, 1235–1247. [CrossRef]
18. Atia, A.A.; Kimura, M. Oxidative Hydroxylation of Aryl Boronic Acid Catalyzed by Co-porphyrin Complexes via Blue-Light Irradiation. *Catalyst* **2020**, *10*, 1262. [CrossRef]
19. Yang, X.; Jiang, X.; Wang, W.; Yang, Q.; Maa, Y.; Wang, K. Catalyst- and solvent-free *ipso*-hydroxylation of arylboronic acids to phenols. *RSC Adv.* **2019**, *9*, 34529. [CrossRef]
20. Borah, R.; Saikia, E.; Bora, S.J.; Chetia, B. Banana pulp extract mediated synthesis of Cu$_2$O nanoparticles: An efficient heterogeneous catalyst for the *ipso*-hydroxylation of arylboronic acids. *Tetrahedron Lett.* **2017**, *58*, 1211–1215. [CrossRef]
21. Elumalai, V.; Hansen, J.H. A scalable and green one-minute synthesis of substituted phenols. *RSC Adv.* **2020**, *10*, 40582. [CrossRef]
22. Molloy, J.J.; Clohessy, T.A.; Irving, C.; Anderson, N.A.; Lloyd-Jones, G.C.; Watson, A.J.B. Chemoselective oxidation of aryl organoboron systems enabled by boronic acid-selective phase transfer. *Chem. Sci.* **2017**, *8*, 1551. [CrossRef]
23. Xu, J.; Wang, X.; Shao, C.; Su, D.; Cheng, G.; Hu, Y. Highly Efficient Synthesis of Phenols by Copper-Catalyzed Oxidative Hydroxylation of Arylboronic Acids at Room Temperature in Water. *Org. Lett.* **2010**, *12*, 1964–1967. [CrossRef]
24. Kim, H.-S.; Joo, S.-R.; Shin, U.S.; Kim, S.-H. Recyclable CNT-chitosan nanohybrid film utilized in copper-catalyzed aerobic *ipso*-hydroxylation of arylboronic acids in aqueous media. *Tetrahedron Lett.* **2018**, *59*, 4597–4601. [CrossRef]
25. Inamoto, K.; Nozawa, K.; Yonemoto, M.; Kondo, Y. Micellar system in copper-catalysed hydroxylation of arylboronic acids: Facile access to phenols. *Chem. Commun.* **2011**, *47*, 11775–11777. [CrossRef]
26. Borah, R.; Saikia, E.; Bora, S.J.; Chetia, B. On-Water synthesis of phenols using biogenic Cu$_2$O nanoparticles without using H$_2$O$_2$. *RSC Adv.* **2016**, *6*, 100443. [CrossRef]
27. Dar, B.A.; Bhatti, P.; Singh, A.P.; Lazar, A.; Sharma, P.R.; Sharma, M.; Singh, B. Clay entrapped Cu(OH)x as an efficient heterogeneous catalyst for *ipso*-hydroxylation of arylboronic acids. *Appl. Catal. A* **2013**, *466*, 60–67. [CrossRef]

28. Bora, S.J.; Chetia, B. Novel CuCl₂-cryptand-[2.2.Benzo] complex: A base free and oxidant free catalyst for *Ipso*-Hydroxylation of aryl/heteroaryl-boronic acids in water at room temperature. *J. Organomet. Chem.* **2017**, *851*, 52–56. [CrossRef]

29. Shin, E.-J.; Kim, H.-S.; Joo, S.-R.; Shin, U.S.; Kim, S.-H. Heterogeneous Palladium–Chitosan–CNT Core–Shell Nanohybrid Composite for Ipso-hydroxylation of Arylboronic Acids. *Catalysis Lett.* **2019**, *149*, 1560–1564. [CrossRef]

30. Duan, P.; Schmidt-Rohr, K. Composite-pulse and partially dipolar dephased multiCP for improved quantitative solid-state ¹³C NMR. *J. Magn. Reson.* **2017**, *285*, 68–78. [CrossRef]

31. Kono, H.; Yunoki, S.; Shikano, T.; Fujiwara, M.; Erata, T.; Takai, M. CP/MAS ¹³C NMR Study of Cellulose and Cellulose Derivatives. *J. Am. Chem. Soc.* **2002**, *9*, 7507. [CrossRef]

32. Idström, A.; Schantz, S.; Sundberga, J.; Chmelka, B.F.; Gatenholm, P.; Nordstierna, L. ¹³C NMR assignments of regenerated cellulose from solid-state 2D NMR spectroscopy. *Carbohydr. Polym.* **2016**, *151*, 480–487. [CrossRef]

33. Zhu, X.; Dai, Y.; Wang, C.; Tan, L. Quantitative and Structure Analysis of Cellulose in Tobacco by ¹³C CP/MAS NMR Spectroscopy. *Beiträge Tab. Int.* **2016**, *27*, 126–135. [CrossRef]

34. Patil, B.H.; Peraje, P.; Naik, D.; Rajaramakrishna, R.; Dittmer, J.; Swamy, S.K.K. Experimental 1H and ¹³C Solid-State NMR Signal Assignment of Paramagnetic Copper (II) 2-Pyrazine-Carboxylate Complex using Density Functional Theory Calculations. *J. Phys. Conf. Ser.* **2021**, *1819*, 012032. [CrossRef]

35. Yuan, C.; Zheng, L.; Zhao, Y. Cu(II)-Catalyzed Homocouplings of (Hetero)Arylboronic Acids with the Assistance of 2-O-Methyl-d-Glucopyranose. *Molecules* **2019**, *24*, 3678. [CrossRef] [PubMed]

36. Yang, H.; Li, Y.; Jiang, M.; Wang, J.; Fu, H. General Copper-Catalyzed Transformations of Functional Groups from Arylboronic Acids in Water. *Chem. Eur. J.* **2011**, *17*, 5652–5660. [CrossRef] [PubMed]

37. Guan, X.; Zhu, H.; Driver, T.G. Cu-Catalyzed Cross-Coupling of Nitroarenes with Aryl Boronic Acids to Construct Diarylamines. *ACS Catal.* **2021**, *11*, 12417–12422. [CrossRef]

38. Bian, Z.; Liu, A.; Li, Y.; Fang, G.; Yao, Q.; Zhange, G.; Wu, Z. Boronic acid sensors with double recognition sites: A review. *Analyst* **2020**, *145*, 719. [CrossRef] [PubMed]